

Available online at www.sciencedirect.com**ScienceDirect**journal homepage: www.elsevier.com/locate/he

Enhancement of redox stability and electrical conductivity by doping various metals on ceria, $\text{Ce}_{1-x}\text{M}_x\text{O}_{2-\delta}$ ($\text{M} = \text{Ni, Cu, Co, Mn, Ti, Zr}$)

Jae-ha Myung ¹, Tae Ho Shin ¹, Xiubing Huang, George Carins,
John T.S. Irvine*

School of Chemistry, University of St. Andrews, Fife, KY16 9ST, United Kingdom

ARTICLE INFO

Article history:

Received 31 December 2014

Received in revised form

29 April 2015

Accepted 4 May 2015

Available online xxx

Keywords:

Ceria

Impedance spectroscopy

Electrical conductivity

Oxide anode

Solid oxide fuel cell

ABSTRACT

Various metal oxide materials have been actively investigated to improve energy efficiency as exhaust-catalyst as well as electrodes in electrochemical devices such as fuel cells, ceramic sensors, photo-catalyst etc. Ceria-based materials are of great interest due to their wide applications; such as redox or oxygen storage promoter in automotive catalyst and solid state conductor in fuel cells. Here we report redox and electrical properties for $\text{Ce}_{1-x}\text{M}_x\text{O}_{2-\delta}$ ($\text{M} = \text{Ni, Cu, Co, Mn, Ti, Zr}$) by X-ray diffraction (XRD) and simultaneous thermo-gravimetric analysis (TGA). Among various system, $\text{Ce}_{1-x}\text{Cu}_x\text{O}_{2-\delta}$ and $\text{Ce}_{1-x}\text{Ni}_x\text{O}_{2-\delta}$ indicated relatively reversible redox behavior, although Cu^{2+} and Ni^{2+} had limited solid solubility in CeO_2 . The enhancement of oxygen carrier concentration and electrical conductivity as well as electrochemical activity in the ceria lattice by the introduction of small amounts transition metal cations have been considered in this study. $\text{Ce}_{0.7}\text{Cu}_{0.3}\text{O}_{2-\delta}$ showed about $1015 \mu\text{mol}[\text{O}_2]/\text{g}$ of oxygen storage capacity (OSC) with high redox stability at 700°C . We also demonstrated that $\text{Ce}_{0.9}\text{Ni}_{0.1}\text{O}_{2-\delta}$ was used as an anode of the YSZ electrolyte supported SOFC single cell; the maximum power density was 0.15 W/cm^2 at 850°C with hydrogen fuel.

Copyright © 2015, The Authors. Published by Elsevier Ltd on behalf of Hydrogen Energy Publications, LLC. This is an open access article under the CC BY license (<http://creativecommons.org/licenses/by/4.0/>).

Introduction

In order to achieve a sustainable future, energy conversion and storage systems with high efficiency and environmentally friendly technology are required. Various metal oxide materials have been actively investigated to improve energy efficiency as exhaust-catalyst as well as electrodes in electrochemical devices such as fuel cells, ceramic sensors,

etc. As the technology matures, parameters such as reliability and durability under severe conditions such as redox, and fuel flexibility become more vital for high efficiency systems. There is therefore an innovative research opportunity for reversible oxide materials for next generation electrochemical devices. Reversible metal/metal oxide systems provide a key entry strategy for next generation energy conversion/storage systems into the current energy economy.

* Corresponding author. Tel.: +44 1334 463800; fax: +44 1334 463808.

E-mail address: jtsi@st-andrews.ac.uk (J.T.S. Irvine).

¹ These authors contributed equally to this work as first author.
<http://dx.doi.org/10.1016/j.ijhydene.2015.05.029>

0360-3199/Copyright © 2015, The Authors. Published by Elsevier Ltd on behalf of Hydrogen Energy Publications, LLC. This is an open access article under the CC BY license (<http://creativecommons.org/licenses/by/4.0/>).

Please cite this article in press as: Myung J-h, et al., Enhancement of redox stability and electrical conductivity by doping various metals on ceria, $\text{Ce}_{1-x}\text{M}_x\text{O}_{2-\delta}$ ($\text{M} = \text{Ni, Cu, Co, Mn, Ti, Zr}$), International Journal of Hydrogen Energy (2015), <http://dx.doi.org/10.1016/j.ijhydene.2015.05.029>

Ceria has the Fluorite structure with space group Fm3m, and it can stably retain this structure under reduction conditions at elevated temperatures even though Ce⁴⁺ would be reduced to Ce³⁺ with an oxygen loss. The amount of lattice oxygen in ceria that can be reversibly exchanged is represented by oxygen storage capacity (OSC) [1]. For that reason, ceria based-solid solutions with controllable particle size and dopant concentrations are also of attractive fundamental significance because of their potential application for oxide ion conduction, exhaust-catalysis, water gas shift (WGS) catalysis, solar cells, three way catalyst, oxygen carrier loop system and solid oxide fuel cells (SOFCs) [2–9]. In particular, not only the OSC but also the electrical conductivity of ceria can be enhanced by isovalent and multi-valent transition metal ion substitution in CeO₂. For example, Fronasiero et al. reported the redox behavior of Ce_{1-x}Zr_xO₂ solid solution and indicated that OSC and redox stability were significantly improved by Zr, doping [10,11]. Ce_{1-x}Cr_xO_{2-δ} was synthesized and the best composition was optimized as Ce_{2/3}Cr_{1/3}O_{2-δ} to give a high OSC material by P. Singh et al. [12].

The interrelation between the ionic radius and redox potential of the dopant element has been widely studied to enhance the oxidation catalytic activity of the doped ceria [13–19]. Balducci et al. demonstrated that the lower reduction energy of the catalyst was effectively related to the larger ionic radius of dopant. Larger dopants tend to facilitate Ce⁴⁺/Ce³⁺ reduction in accord with the increase in ionic size associated with the Ce reduction (radius Ce³⁺ = 1.143 Å and Ce⁴⁺ = 0.97 Å) [18,19]. For certain noble metals such as Pt, Pd, Cu and Rh, calculation also shows a significant lowering of the calculated reduction energy [20]. Andersson et al., also reported that the reducibility of doped ceria (Si, Ge, Sn and Pb) was enhanced with decreasing ionic radius. From their results, however, some dopants did not follow this dependency on the ionic radius and this indicates that e.g. influences on the electronic structure from the dopant are also important factors in lowering the reduction energy. It is obviously instructive to consider the effect of the driving force of the electronic structure of the dopant, and the effect of the ionic size for the design of next generation reversible oxide storage materials. Here we investigate the redox behavior of various doped cerias using simultaneous thermo-gravimetric analysis (TGA) and electrical conductivity measurement on redox cycling. With this information, one can monitor the stability and electrical properties of doped ceria. Ce_{1-x}M_xO_{2-δ} (M = Ni, Cu, Co, Mn, Ti, Zr) were investigated and both the redox properties related with OSC and electrical conductivity were considered when screening a suitable dopant for ceria. Ni and Cu have been widely used for the conventional SOFC anode materials as the mixture with YSZ (8 mol% Yttria Stabilized Zirconia) and GDC (10 mol % Gadolinium Doped Ceria), but these metals are usually used above 40 wt% of the total anode amount and easily coarsened and agglomerated at high temperature. For applying the nano-sized metals on YSZ back skeleton, infiltration methods are widely employed, although these may still undergo coarsening and agglomeration of the metal particles due to the high operating temperature. In our study, Ce_{0.9}Cu_{0.1}O₂ and Ce_{0.9}Ni_{0.1}O₂ showed high redox stability and

OSC, and were also applied as the SOFC anode to analyze their electrochemical activity for hydrogen oxidation in an electrolyte supported single cell.

Experimental

Preparation of powders

For a preparation for doped ceria powders of Ce_{1-x}M_xO₂ (M = Ni, Cu, Co, Mn, Ti, Zr), nitrate precursors was mixed in a beaker with 100 ml deionized-water and then this solution was heated on a hotplate to dryness from Ce(NO₃)₃·6H₂O (99.9%, Sigma–Aldrich Co. LLC, UK), Ni(NO₃)₂·6H₂O (99%, Alfa Aesar, USA), Cu(NO₃)₂·3H₂O (99%, Sigma–Aldrich Co. LLC, UK), Zr(NO₃)₂·XH₂O (99%, Aldrich Co. LLC, UK), Co(NO₃)₂·6H₂O (99%, Sigma–Aldrich Co. LLC, UK), C₆H₁₈N₂O₈Ti (Sigma–Aldrich Co. LLC, UK.) and Mn(NO₃)₂·6H₂O (98%, Alfa Aesar, USA). After this, the ashes were fired to fully remove nitrate at 350 °C and its powder was calcined at 400 °C for 2 h and 700–1000 °C for 6 h, respectively for crystallization. The resulting powder was then ground, re-pressed and fired at 1300 °C for 5 h for measuring the electrical conductivity.

Fabrication of single cells

The electrolyte supported single cells were employed to measure their electrochemical activity with hydrogen fuel. The YSZ powder was pressed into pellets and fired in air at 1500 °C for another 12 h to obtain a dense support.

The screen printing inks were prepared by de-agglomerating the doping ceria powder as an anode material using planetary ball milling in α-terpineol with 10 wt% of Hypermer KD1 dispersant (Uniqema). After this step, the de-agglomerated slurry was added to an ink vehicle, consisting of 15 wt% PVB (polyvinyl butyral, Butvar, Sigma–Aldrich) in α-terpineol. This mixture was mixed by planetary ball milling again. This ink was screen-printed onto a dense YSZ support (500 μm) with thickness of 100 μm and fired at 1200 °C for 3 h. LSCF-GDC cathodes were prepared with above method and fired at 1000 °C for 2 h. In these button cells, both anode and cathode had a surface area of 1 cm².

Characterization methods

The crystalline phase was identified by using X-ray diffraction (XRD, PANalytical Empyrean diffractometer, Netherlands) with reflection mode using Cu Kα radiation. The diffraction data were refined by the Rietveld method, using the program General Structure Analysis System (GSAS) and STOE Win XPOW. Thermal gravimetric analysis (TGA, NETZSCH TG 209, NETZSCH Geraetebau GmbH, Germany) was carried out with a heating & cooling rate of 10 °C/min to evaluate the oxygen loss and accommodation on redox cycling in air/5% H₂ in the compositions synthesized. Electrical conductivity was measured on the sintered pellets by the standard four terminal DC methods or Van Der Pauw method up to 850 °C in ambient air. A current of 100 mA (model: Keithley 220, Keithley Instruments Inc., U.S.A.) was applied in both directions, and resistance was calculated as a gradient of

potential vs. current. For the measurement of single cells with hydrogen fuel from 650 °C to 850 °C, IV and impedance data between 105 Hz and 0.1 Hz were recorded using an IM6 and ZENNIUM workstation (Zahner-Elektrik GmbH & Co.KG, Germany).

Results and discussion

The calcined powders of $\text{Ce}_{1-x}\text{M}_x\text{O}_{2-\delta}$ ($\text{M} = \text{Ni}, \text{Cu}, \text{Co}, \text{Mn}, \text{Ti}, \text{Zr}$) ($0 \leq x \leq 0.1$) were obtained as a fluorite crystalline phase of space group $\text{Fm}3m$. Fig. 1 shows the XRD patterns of 0.1 mol doped ceria $\text{Ce}_{0.9}\text{M}_{0.1}\text{O}_{2-\delta}$ ($\text{M} = \text{Ni}, \text{Cu}, \text{Co}, \text{Mn}, \text{Ti}, \text{Zr}$) calcined at 1000 °C and there were no significant secondary peaks. Structural parameters of $\text{Ce}_{1-x}\text{M}_x\text{O}_{2-\delta}$ ($\text{M} = \text{Ni}, \text{Cu}, \text{Co}, \text{Mn}$) ($x = 0.1$) are presented in Table 1 and Fig. 2. Since the substitution of $2^{+}/3^{+}$ smaller valence dopants ($\text{M} = \text{Ni}, \text{Cu}, \text{Co}, \text{Mn}$) for Ce^{4+} (ionic radius = 0.97 Å) in $\text{Ce}_{1-x}\text{M}_x\text{O}_{2-\delta}$, slightly decrease lattice parameters in accord with smaller charge valence of transition metal dopant than 4+ valance of Ce. Broadly, the lattice constants as ionic radius increase; however, shows almost constantly linear as shown in Fig. 2. It suggests that oxygen content are probably more important oxygen vacancies created by doping and lead to an increase in lattice parameters due to the loss of $\text{M}(\text{Ce})-\text{O}$ bonding length [21–27]. In any case, all lattice parameters of $\text{Ce}_{1-x}\text{M}_x\text{O}_{2-\delta}$ ($\text{M} = \text{Ni}, \text{Cu}, \text{Co}, \text{Mn}$) ($0 \leq x \leq 0.1$) deviate in accord with ionic radius from that of 5.41103 Å of

pure ceria [28], suggesting that above metal dopants are soluble in ceria lattice.

In addition, because of lower redox couple potential of Cu, and Ni compared to $\text{Ce}^{4+}/\text{Ce}^{3+}$ (1.61 V) as shown in Table 1, these divalent metal dopants may give a synergistic interaction for oxygen storage and regenerate between Ce ORR and dopant redox potential. Consequently, Cu, Ni and Co doped ceria show good stability during redox cycling testing as potential candidate materials related with OSC application in this study.

For redox cycling tests, a powder calcined at 700 °C was exposed alternately to air and 5% H₂ during TGA analysis. In particular, the Cu doped material shows more stable redox cycling and higher oxygen capacity behavior than others up to 700 °C. As shown in Fig. 3a, the ranking of performance, i.e. $\text{Ti} \ll \text{Mn} < \text{Cu} \leq \text{Ni} < \text{Co}$, for the OSC of $\text{Ce}_{0.9}\text{M}_{0.1}\text{O}_{2-\delta}$ approximately correlates with the decreasing order of lattice volumes [29]. It might be explained by considering that the reducibility of doped ceria was enhanced with the decreasing ionic radius and oxygen defect formation energy would be closely related with lattice distortion from not only various dopant ionic radius size but also redox couple potential. It seems more likely that related factors determine the lattice volume and OSC, rather than a direct relationship existing. Furthermore, Fig. 3b shows TGA analysis of $\text{Ce}_{1-x}\text{Cu}_x\text{O}_{2-\delta}$ ($x = 0.1, 0.2, 0.3$ mol% in ceria) during redox cycle at 700 °C and an OSC value was improved to 1015 from 343.75 μmol [O₂]/g at 700 °C by increasing the amount of Cu (0.1–0.3 mol%) in ceria.

To confirm the electrochemical stability, electrical properties of $\text{Ce}_{1-x}\text{M}_x\text{O}_{2-\delta}$ ($\text{M} = \text{Mn}, \text{Ti}, \text{Cu}, \text{Ce}, \text{Ni}$) were measured and Fig. 4 shows its electrical conductivity as a function of various metal dopants in ceria.

Accordingly, small metal dopants exhibited little influence on conductivity but Zr⁴⁺ and Ti⁴⁺, isovalent type dopants, gave rise to a slight increase in ceria conductivity and activation energy was close to 1.42 eV for CeO_2 reference sample. However, isovalent type doped $\text{Ce}_{0.9}\text{M}_{0.1}\text{O}_{2-\delta}$ for $\text{M} = \text{Zr}, \text{Ti}$ shows 1.19 and 0.88 eV, respectively. On the other hand, transition metal doped ceria, Mn shows also much decreased value with 1.05 eV but bivalent doped Cu and Ni shows slightly increased activation energy with 1.45 eV and 1.44 eV respectively even though there were no much effect on their total conductivity. The addition of dopant cations in ceria decreases the activation energy for oxygen vacancy diffusion.

This decrease may be due to the break-up of attractive interactions between dopant cations and oxygen defect formation. Among various metals as dopants in ceria, aliovalent metals; Cu, Ni and Mn show reasonable electrical

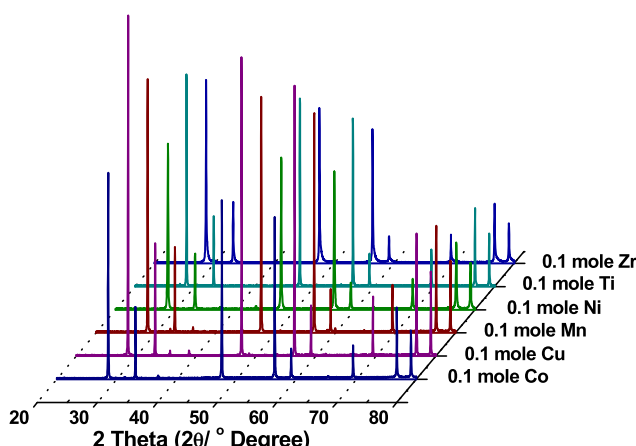


Fig. 1 – Powder XRD patterns of $\text{Ce}_{1-x}\text{M}_x\text{O}_{2-\delta}$ ($\text{M} = \text{Ni}, \text{Cu}, \text{Co}, \text{Mn}, \text{Ti}, \text{Zr}$) ($0 \leq x \leq 1$), synthesized 1000 °C for 6 h.

Table 1 – Lattice parameter of $\text{Ce}_{0.9}\text{M}_{0.1}\text{O}_{2-\delta}$ ($\text{M} = \text{Co}, \text{Ni}, \text{Cu}, \text{Mn}$) calcined in air at 1000 °C.

Compounds	Ionic radius (M) (Å)	Lattice parameter (a/Å)	Lattice volume (Å ³)	Redox couple potential (V)
$\text{Ce}_{0.9}\text{Co}_{0.1}\text{O}_{2-\delta}$	0.65 [23,25]	5.411129 (02)	158.4396 (01)	1.92 V/Co ^{3+/2+}
$\text{Ce}_{0.9}\text{Ni}_{0.1}\text{O}_{2-\delta}$	0.69 [25,26]	5.411092 (29)	158.4363 (15)	0.257 V/Ni ^{2+/0}
$\text{Ce}_{0.9}\text{Cu}_{0.1}\text{O}_{2-\delta}$	0.73 [22,25]	5.41172 (05)	158.4913 (27)	0.340 V/Cu ^{2+/0}
$\text{Ce}_{0.9}\text{Mn}_{0.1}\text{O}_{2-\delta}$	0.96 [24,25]	5.41174 (25)	158.4932 (13)	1.5 V/Mn ^{3+/2+}
$\text{CeO}_2-\delta$	—	5.41103 (05)	158.4311 (25)	

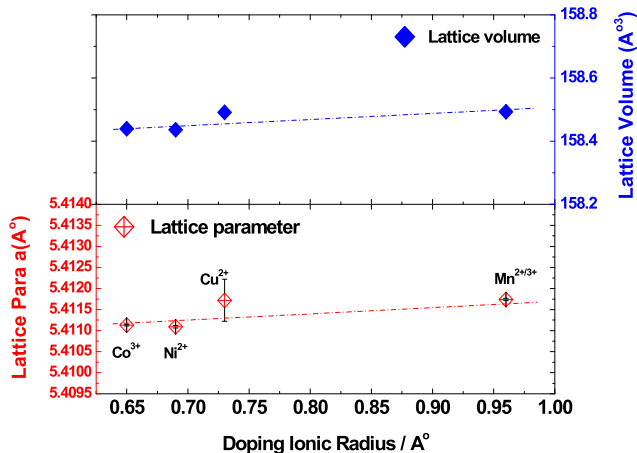


Fig. 2 – Structural parameters of $\text{Ce}_{0.9}\text{M}_{0.1}\text{O}_{2-\delta}$ ($\text{M} = \text{Ni}, \text{Cu}, \text{Co}, \text{Mn}$) calcined at 1000 °C as a function of the dopant ionic radius.

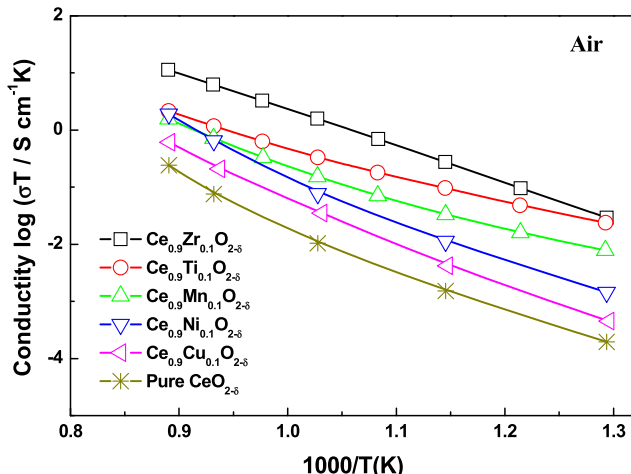


Fig. 4 – Electrical conductivities of $\text{Ce}_{1-x}\text{M}_x\text{O}_{2-\delta}$ ($\text{M} = \text{Zr}, \text{Mn}, \text{Ti}, \text{Cu}, \text{Ni}$) ($0 \leq x \leq 0.1$) in air with elevated temperature up to 900 °C.

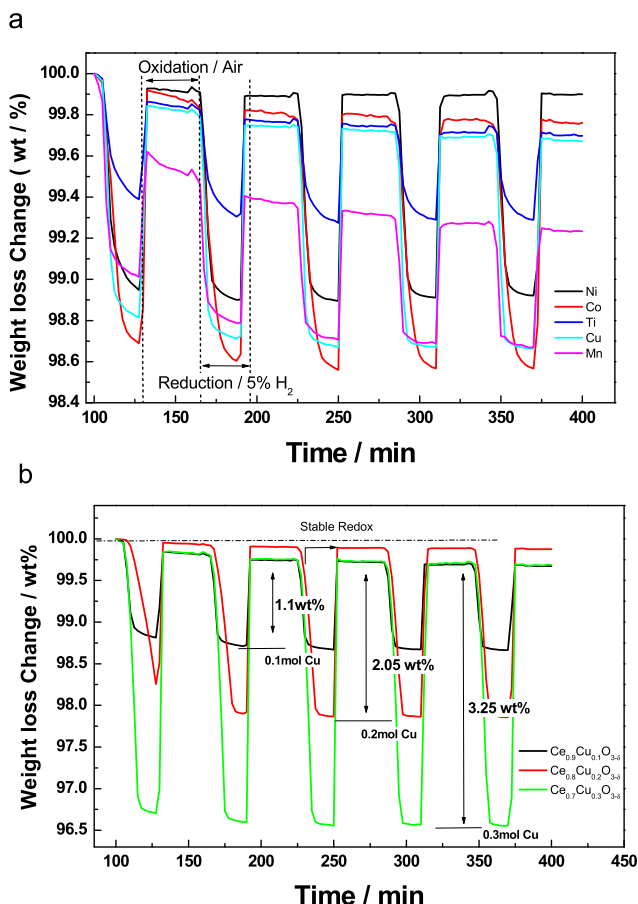


Fig. 3 – TGA analysis of during redox cycle $\text{Ce}_{1-x}\text{M}_x\text{O}_{2-\delta}$ ($\text{M} = \text{Ni}, \text{Cu}, \text{Co}, \text{Mn}, \text{Ti}, \text{Zr}$) ($0 \leq x \leq 0.3$), exposed to air and 5% H_2 repeatedly; weight changing of $\text{Ce}_{0.9}\text{M}_{0.1}\text{O}_{2-\delta}$ ($\text{M} = \text{Ni}, \text{Co}, \text{Ti}, \text{Cu}, \text{Mn}$) under redox 5 cycles (a), TGA analysis of $\text{Ce}_{1-x}\text{Cu}_x\text{O}_{2-\delta}$ ($0 \leq x \leq 0.3$) during redox (b).

conductivity and a higher amount of lattice oxygen as OSC materials that can be reversibly exchanged from CeO_2 . On the other hand, for some transition metals including Mn, however, reversibility in redox cycle seems poorer than the Cu and Ni doped one. $\text{Ce}_{0.9}\text{M}_{0.1}\text{O}_{2-\delta}$ ($\text{M} = \text{Ni}, \text{Cu}$) were closed to single phases, high redox stability and high OSC which would be employed on solid oxide fuel cell as an anode.

Fig. 5 shows the cell performance and impedance spectra of $\text{CeO}_2/\text{YSZ}/\text{LSCF-GDC}$, $\text{Ce}_{0.9}\text{Cu}_{0.1}\text{O}_{2-\delta}/\text{YSZ}/\text{LSCF-GDC}$ and $\text{Ce}_{0.9}\text{Ni}_{0.1}\text{O}_{2-\delta}/\text{YSZ}/\text{LSCF-GDC}$ single cells with hydrogen fuel. The performance of CeO_2 anode was 4.1 mW/cm² at 850 °C. However, the potential curves were not stable over all temperatures due to extremely low catalytic activity. The low catalytic activity seemed not only to affect the absorption and transfer between hydrogen molecule and ions on CeO_2 , but also the redox coupling reaction of pure ceria anode with unstable partial oxygen pressure (P_{O_2}) of the anode surface. $\text{Ce}_{0.9}\text{Cu}_{0.1}\text{O}_{2-\delta}$ was also showed slightly unstable potential curves possibly caused by phase decomposition by a low solubility of Cu in CeO_2 at high temperature, while the performances were higher than that of pure CeO_2 anode. In the case of $\text{Ce}_{0.9}\text{Ni}_{0.1}\text{O}_{2-\delta}$ anode, the doping with Cu or Ni metals stabilized the Ceria reduction and increased the electrochemical activity for hydrogen reduction. The anode of SOFCs is generally modeled as an equivalent parallel circuit composed with a resistor and a constant phase element (CPE). The polarization resistance is further divided in to high and low frequency polarization resistances, the resistance at high frequency ($f_{\text{max}} = 2.03$ kHz) is influenced by the transport of charged species and the gas diffusion and low frequency ($f_{\text{max}} = 0.89$ Hz) is related to the catalytic activity for the oxidation of hydrogen. $\text{Ce}_{0.9}\text{Ni}_{0.1}\text{O}_{2-\delta}$ anodes showed much smaller polarization resistance at high and low frequencies, in particular, incredibly improved the electrochemical activity of hydrogen comparing with $\text{Ce}_{0.9}\text{Cu}_{0.1}\text{O}_{2-\delta}$ and pure CeO_2 , which was matching with conventional Ni or Cu cermet SOFCs. The high temperature

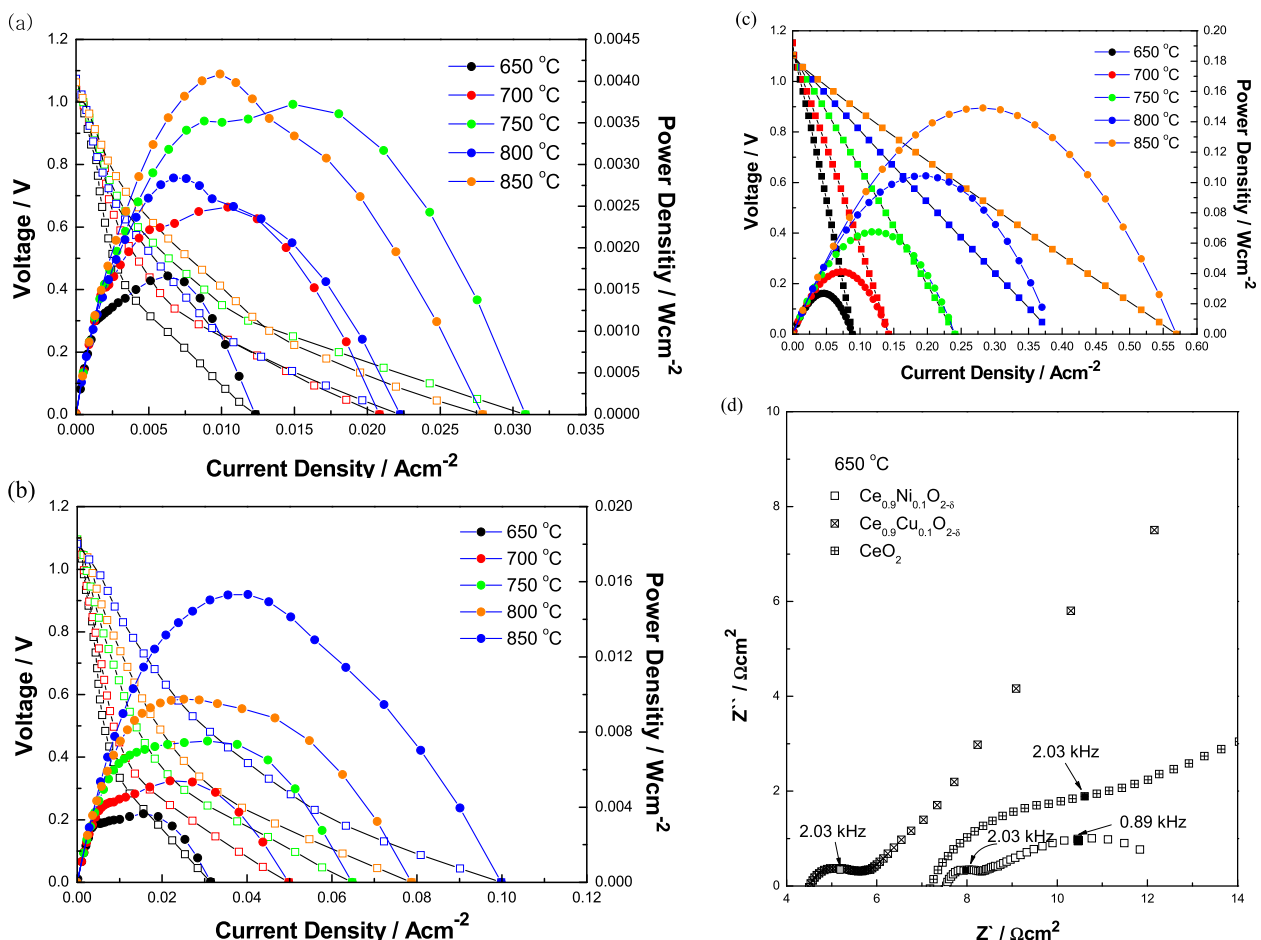


Fig. 5 – IV curves of Ce_{1-x}M_xO_{2-δ} (Cu, Ni) (0 ≤ x ≤ 0.1) anode/YSZ electrolyte/LSCF-GDC cathode single cells in hydrogen from 650 °C to 850 °C; CeO₂ (a), Ce_{0.9}Cu_{0.1}O_{2-δ} (b), and Ce_{0.9}Ni_{0.1}O_{2-δ} (c), and impedance spectra at 650 °C (d).

formation of the electrode (over 1200 °C) may cause partial exsolution of NiO particles from the Ce_{0.9}Ni_{0.1}O_{2-δ} lattice. However, the exsolved NiO could increase the catalyst active area and increase the electrical conductivity.

Conclusion

The aliovalent metal solubility in ceria was not so high to synthesize single phase ceria lattice with e.g. 20% metal substitution. However, a small amount of doping among various ceria systems shows high potential for application in quite stable redox behavior and improving electrical conductivity. In particular, divalent small sized cations such as Cu show higher potential for OSC application because of lower ionic radius and lower redox potential. Herein, we reported reasonable OSC value achieved with Cu doped ceria and it would also have potential as an electrode catalyst of electrochemical devices. Consequently, this study reveals that Cu²⁺ substituted ceria can be another promising candidate for higher OSC materials as well as electrochemical catalyst; exhaust three way catalyst, catalyst for methane and CO oxidation catalyst. Also, Ni²⁺ substituted ceria showed high electrochemical activity as SOFC anode, high OSC value as well with good redox stability.

Acknowledgments

This work was supported by EPSRC (EP/I022570/1, EP/K015540/1, EP/I038950/1, EP/K021036/1).

REFERENCES

- [1] Yao HC, Yao YFY. Ceria in automotive exhaust catalysts: I. Oxygen storage. *J Catal* 1984;86:254–65.
- [2] Fu Q, Saltsburg H, Flytzani-Stephanopoulos M. Active nonmetallic Au and Pt species on ceria-based water-gas shift catalysts. *Science* 2003;301:935–8.
- [3] Wang X, Rodriguez JA, Hanson JC, Gamarra D, Martínez-Arias A, Fernández-García M. In situ studies of the active sites for the water gas shift reaction over Cu–CeO₂ catalysts: complex interaction between metallic copper and oxygen vacancies of ceria. *J Phys Chem B* 2005;110:428–34.
- [4] Corma A, Atienzar P, Garcia H, Chane-Ching J-Y. Hierarchically mesostructured doped CeO₂ with potential for solar-cell use. *Nat Mater* 2004;3:394–7.
- [5] Reddy BM, Bharali P, Saikia P, Khan A, Lordin S, Muhler M, et al. Hafnium doped ceria nanocomposite oxide as a novel redox additive for three-way catalysts. *J Phys Chem C* 2007;111:1878–81.

- [6] Hedayati A, Azad A-M, Rydén M, Leion H, Mattisson T. Evaluation of novel ceria-supported metal oxides as oxygen carriers for chemical-looping combustion. *Ind Eng Chem Res* 2012;51:12796–806.
- [7] Shin TH, Ida S, Ishihara T. Doped $\text{CeO}_2\text{-LaFeO}_3$ composite oxide as an active anode for direct hydrocarbon-type solid oxide fuel cells. *J Am Chem Soc* 2011;133:19399–407.
- [8] Shin TH, Vanalabhpata P, Ishihara T. Oxide composite of $\text{Ce}(\text{Mn},\text{Fe})\text{O}_2$ and $\text{La}(\text{Sr})\text{Fe}(\text{Mn})\text{O}_3$ for anode of intermediate temperature solid oxide fuel cells using LaGaO_3 electrolyte. *J Electrochem Soc* 2010;157:B1896–901.
- [9] Ishihara T, Shin TH, Vanalabhpata P, Yonemoto K, Matsuka M. $\text{Ce}_{0.6}(\text{Mn}_{0.3}\text{Fe}_{0.1})\text{O}_2$ as an oxidation-tolerant ceramic anode for SOFCs using LaGaO_3 -based oxide electrolyte. *Electrochem Solid-State Lett* 2010;13:B95–7.
- [10] Fornasiero P, Dimonte R, Rao GR, Kaspar J, Meriani S, Trovarelli A, et al. Rh-loaded $\text{CeO}_2\text{-ZrO}_2$ solid-solutions as highly efficient oxygen exchangers: dependence of the reduction behavior and the oxygen storage capacity on the structural-properties. *J Catal* 1995;151:168–77.
- [11] Monte RD, Kaspar J. Nanostructured $\text{CeO}_2\text{-ZrO}_2$ mixed oxides. *J Mater Chem* 2005;15:633–48.
- [12] Singh P, Hegde MS, Gopalakrishnan J. $\text{Ce}_x/3\text{Cr}_1/3\text{O}_{2+y}$: a new oxygen storage material based on the fluorite structure. *Chem Mater* 2008;20:7268–73.
- [13] Andersson DA, Simak SI, Skorodumova NV, Abrikosov IA, Johansson B. Theoretical study of CeO_2 doped with tetravalent ions. *Phys Rev B* 2007;76:174119.
- [14] Cao L, Ni C, Yuan Z, Wang S. Correlation between catalytic selectivity and oxygen storage capacity in autothermal reforming of methane over $\text{Rh}/\text{Ce}_{0.45}\text{Zr}_{0.45}\text{RE}_{0.1}$ catalysts ($\text{RE} = \text{La, Pr, Nd, Sm, Eu, Gd, Tb}$). *Catal Commun* 2009;10:1192.
- [15] Parthasarathi B, Mitra S, Sampath S, Hegde MS. Promoting effect of CeO_2 in a Cu/CeO_2 catalyst: lowering of redox potentials of Cu species in the CeO_2 matrix. *Chem Commun* 2001:927.
- [16] Reddy BM, Bharali P, Saikia P, Park SE, van den Berg MWE, Muhler M, et al. Structural characterization and catalytic activity of nanosized $\text{Ce}_x\text{M}_{1-x}\text{O}_2$ ($\text{M} = \text{Zr \& Hf}$) mixed oxides. *J Phys Chem C* 2008;112:11729.
- [17] Tang XL, Zhang BC, Li Y, Xu YD, Xin Q, Shen WJ. CuO/CeO_2 catalysts: redox features and catalytic behaviors. *Appl Catal A* 2005;288:116.
- [18] Balducci G, Islam MS, Kašpar J, Fornasiero P, Graziani M. Reduction process in $\text{CeO}_2\text{-MO}$ and $\text{CeO}_2\text{-M}_2\text{O}_3$ mixed oxides. *Chem Mater* 2003;15:3781.
- [19] Balducci G, Islam MS, Kašpar J, Fornasiero P, Graziani M. Bulk reduction and oxygen migration in ceria-based oxides. *Chem Mater* 2000;12:677.
- [20] Kehoe AB, Scanlon DO, Watson GW. Role of lattice distortions in the oxygen storage capacity of divalent-doped CeO_2 . *Chem Mater* 2011;23:4464–8.
- [21] Heo NH, Cruz-Patalinghug WV, Seff K. Crystal structure of zeolite 4A ion exchanged to the limit of its stability with nickel(II). *J Phys Chem* 1986;90:3931–5.
- [22] Rives V, Kannan S. Layered double hydroxides with the hydrotalcite-type structure containing Cu, Ni and Al. *J Mater Chem* 2000;10:489–95.
- [23] Kashiwagi T, Nakayama M, Watanabe K, Wakihara M, Kobayashi Y, Miyashiro H. Relationship between the electrochemical behavior and Li arrangement in $\text{Li}_x\text{M}_{2-y}\text{O}_4$ ($\text{M} = \text{Co, Cr}$) with spinel structure. *J Phys Chem B* 2006;110:4998–5004.
- [24] Lufaso MW, Woodward PM, Goldberger J. Crystal structures of disordered $\text{A}_2\text{Mn}^{3+}\text{M}^{5+}\text{O}_6$ ($\text{A} = \text{Sr, Ca}; \text{M} = \text{Sb, Nb, Ru}$) perovskites. *J Solid State Chem* 2004;177:1651–9.
- [25] Shannon R. Revised effective ionic radii and systematic studies of interatomic distances in halides and chalcogenides. *Acta Crystallogr Sect A* 1976;32:751–67.
- [26] Sohn J-H. Microwave dielectric characteristics of ilmenite-type titanates with high Q values. *Jpn J Appl Phys Part 2 Lett* 1994;33:5466–70.
- [27] Norberg ST, Hull S, Eriksson SG, Ahmed I, Kinyanjui F, Biendicho JJ. Pyrochlore to fluorite transition: the $\text{Y}_2(\text{Ti}_{1-x}\text{Zr}_x)_2\text{O}_7$ ($0.0 \leq x \leq 1.0$) system. *Chem Mater* 2012;24:4294–300.
- [28] Ramesh S, James Raju KC. Preparation and characterization of $\text{Ce}_{1-x}(\text{Gd}_{0.5}\text{Pr}_{0.5})_x\text{O}_2$ electrolyte for IT-SOFCs. *Int J Hydrogen Energy* 2012;37:10311.
- [29] Mai H-X, Sun L-D, Zhang Y-W, Si R, Feng W, Zhang H-P, et al. Shape-selective synthesis and oxygen storage behavior of ceria nanopolyhedra, nanorods, and nanocubes. *J Phys Chem B* 2005;109:24380–5.